An Assessment of Heave Response Dynamics for Electrically Driven Rotors of Increasing Diameter

Ariel Walter PhD Student
Michael McKay PhD Student
Robert Niemiec Research Scientist
Farhan Gandhi Redfern Chair in Aerospace Engineering
Colin Hamilton Undergraduate Research Assistant

Center for Mobility with Vertical Lift (MOVE)
Rensselaer Polytechnic Institute
Troy, NY United States

Chris Jaran
Chief Executive Officer
Terrafugia
Woburn, MA, United States

ABSTRACT

An examination is conducted of the effects of increasing rotor size on system heave response time and power consumption, due to the increasing rotor blade inertia. The study aims to establish a rotor size at which using an electric motor and fixed-pitch, variable-RPM rotor may no longer be feasible due to the degradation in system climb rate response time and handling qualities ratings. Several isolated rotors ranging from 1 to 8 feet in diameter are simulated, and the heave responses are examined based on Froude scaled ADS-33E-PRF requirements. A model validation is performed using data from a 28-inch diameter rotor tested on a rotor test stand apparatus. Various feedback controller designs are then considered, including proportional and proportional-derivative control laws. Pure proportional control fails to reach scaled Level 1 requirements due to the underutilization of the motor. Using proportional-derivative control, rotors 6 feet or less in diameter can meet the scaled ADS-33E-PRF Level 1 heave response requirements with variable-RPM control alone; rotors larger than this may not be responsive enough for effective operation.

NOTATION

F	=	Froude Scaling Factor
w	=	Heave Rate (ft/s)
K	=	Final Value of Step Response (ft/s)
t	=	Time (s)
τ	=	Time Delay (s)
T	=	Time Constant (s)
I	=	Rotor Rotational Inertia ($slug * ft^2$)
P	=	Motor Power (hp)
τ_{aero}	=	Aerodynamic Torque
Ω	=	Rotor Rotational Speed (RPM)
T_{rotor}	=	Rotor Thrust
D	=	Rotor Diameter (ft)

Presented at the 2019 Autonomous VTOL Technical Meeting and eVTOL Symposium, Mesa, AZ, Jan 29-31, 2019

INTRODUCTION

The Urban Air Mobility Grand Challenge put forward by NASA (Ref. 1) reflects a growth in interest and development of larger-scale electric VTOL (eVTOL) aircraft, which are currently being considered for a variety of future applications as air transport vehicles for both cargo and passengers. Additionally, Uber issued a call for participation in the design and development of VTOL air taxis (Ref. 2) for passenger transport between cities and suburbs. The scale of these transport aircraft would be significantly larger than the multicopters that are currently commercially available (typically less than 50 lb gross weight).

Many challenges to scaling up eVTOL from their current size exist, some of which are highlighted by Johnson et al. (Ref. 3), who identified several key research areas necessary for the development of air taxis, including operational effectiveness, safety, and performance. Related to these areas are the aircraft handling qualities, which are effectively a quantification of the responsiveness and maneuverability of the aircraft.

Most eVTOL aircraft utilize fixed-pitch, variable-RPM rotors

to regulate the thrust and moments on the aircraft, which ties the maneuverability of the aircraft to the rate at which the rotors' speeds can be changed. The increasing rotational inertia of larger rotor blades will cause a greater delay between a commanded and actual change in rotor speed, reducing the agility of multicopters that rely on few, large rotors.

Though well-established for traditional helicopters, handling qualities metrics for evaluating multicopters are still in the process of being refined. Several different groups have attempted to define handling qualities metrics for multi-rotor aircraft. In the current literature, there are studies that provide simple scaling of existing military specifications (Refs. 4, 5), seek to define/develop new handling qualities criteria and evaluation methodology (Refs. 6, 7), as well as provide a redefinition of the existing Cooper-Harper rating scale (Ref. 8). Also, Klyde et al. (Ref. 9) suggest a process to define UAV handling qualities guided by existing military specifications that are altered depending on the weight and associated mission tasks or use cases for the aircraft.

Ivler et al. (Ref. 4) utilized a scaled version of the ADS-33E-PRF (Ref. 10) Mission Task Elements (MTEs) to evaluate the performance of a 3.75 lb quadcopter, and concluded that kinematically scaled (based on the maximum speed of the aircraft) ADS-33E-PRF requirements are an effective way to quantitatively evaluate handling qualities for the quadcopter.

Kinematic scaling cannot be utilized if the maximum flight speed of the aircraft is unknown. However, Froude-scaled MTEs based on the length scaling of the aircraft (Ref. 5) provide another option. The Froude-scaling described by Alverenga et al. (Ref. 5) uses relative length scales to change the upper bounds of level 1 and level 2 handling qualities. The time constant and delay are multiplied by F, which is the square root of the diagonal hub-to-hub distance of the quadcopter divided by the UH-60 rotor diameter (Eq. 1).

$$F = \sqrt{\frac{\text{Hub-to-Hub Distance}}{\text{UH-60 Rotor Diameter}}} \tag{1}$$

Consider the hover and low speed requirement of height response characteristics to a collective control input in the ADS-33E-PRF. For this MTE, the response of the aircraft to a step change in commanded climb rate is fit by a first-order transfer function, in the form of Eq. 2. The two parameters T and τ represent the time constant and delay of the first-order response, and are used to parameterize the fit, while the value of K is fixed by the size of the step change in climb rate. The T and τ which result in the best fit to the simulation (or experimental data) is compared to the level 1 and level 2 bounds given in Table 1.

$$w_{est}(t) = K[1 - exp(-\frac{t-\tau}{T})] \tag{2}$$

Table 1. Heave Rate Response Requirements

Level	Time Constant T (s)	Time Delay τ (s)
1	5.0	0.20
2	∞	0.30

MODELING

In this study, isolated rotors ranging from 1 to 8 feet in diameter are simulated. The rotor response to a collective control input is examined through the simulated heave rate response of the system. This response is then compared to the Froude-scaled (based on length) ADS-33E-PRF boundaries.

Scaling of Heave Handling Qualities Metrics

As described, the method developed in Ref. 5 with the Froude scaling factor in Eq. 1 will be utilized to scale ADS-33E-PRF handling qualities metrics for the multi-rotor aircraft. Based on the geometry of the AeroQuad Cyclone (Fig. 1), a representative 2 kg quadcopter with 12 inch diameter rotors and a hub-to-hub distance of 24 inches, twice the rotor diameter is used to approximate the hub-to-hub distance for a rotor of arbitrary size. Thus, Eq. 1 becomes Eq. 3.

$$F_{\text{isolated}} = \sqrt{\frac{2(\text{Quadcopter Rotor Diameter})}{\text{UH-60 Rotor Diameter}}} \tag{3}$$

Rotor Parameters

The geometry of the simulated rotor is based on the AeroQuad Cyclone quadcopter (Fig. 1). The nominal specifications of the Cyclone rotors are given in Table 2. The blades are assumed to have a linear twist and linear taper. As the rotor diameter is scaled up in simulation, the chord length is appropriately scaled to maintain the solidity and taper ratio.

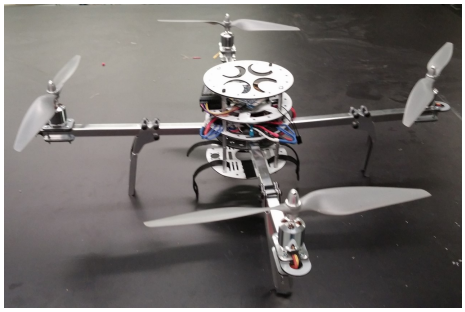

Fig. 1. AeroQuad Cyclone Quadcopter

Table 2. Nominal Rotor Parameters

Parameter	Value
Rotor Diameter	12 in
Root Airfoil	NACA 4412
Tip Airfoil	Clark Y
Root Chord	0.866 in
Tip Chord	0.343 in
Root Pitch	21.5°
Tip Pitch	11.1°
Rotor Solidity	0.09
Rotor Mass	0.049 lbm

Rotor & Motor Inertia Calculations

CAD models of several multicopter rotors were used to compute the rotational inertia, assuming the rotors were made out of carbon fiber reinforced polymer. A curve was then fit to these data points (Fig. 2) in order to find an approximation of rotor inertia as a function of rotor diameter (Eq. 4), where D is measured in feet, and the inertia is in slug ft^2.

$$I_{rotor} = 4.8 \times 10^{-5} D^5 \tag{4}$$

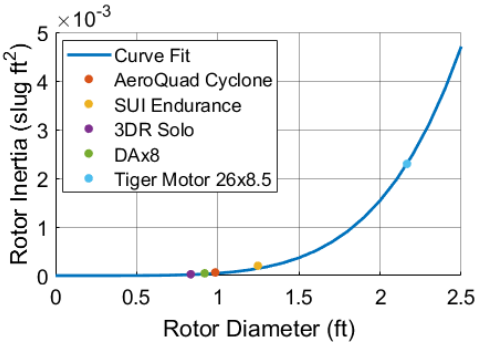

Fig. 2. Estimation of Rotor Rotational Inertia

Motor inertia was computed for several electric motors by taking measurements of the mass, thickness, outer diameter, and height of the rotating part of the motor. The motor inertia was then calculated assuming it was a hollow steel cylinder. Equation 6 was used to map the rated power of the motor to an appropriate rotor diameter and generate the data points in Fig. 3. Fitting a curve to these points yields Eq. 5, where diameter and inertia are measured in ft and slug ft^2, respectively.

$$I_{motor} = 6.8 \times 10^{-6} D^2 \tag{5}$$

In the rotor-motor system, the rotational inertia of the rotor is dominant. Even for the smallest rotor being considered (1 ft diameter) the predicted rotor rotational inertia is around 90% of the total system inertia, shown in Fig. 4. Therefore, the inertia of the motor is neglected, and the rotational inertia of the rotor-motor system is assumed to be equal to the rotational inertia of the rotor.

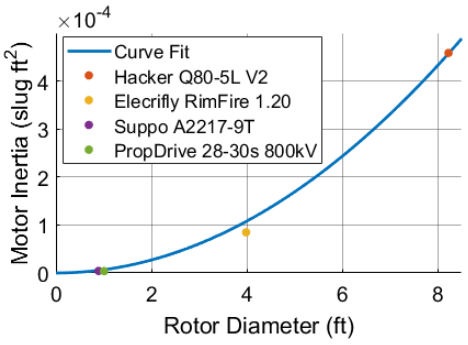

Fig. 3. Estimation of Motor Rotational Inertia

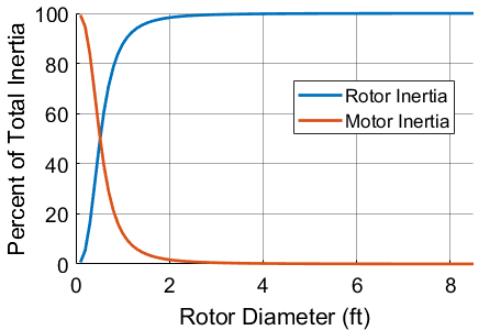

Fig. 4. Estimated Rotor and Motor Inertia as Percent of Total

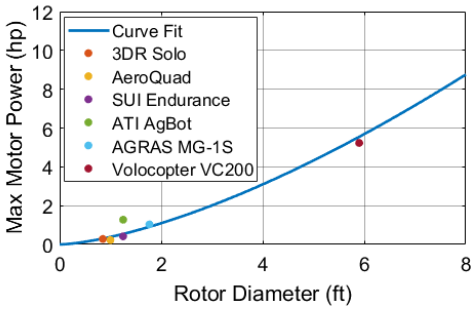

Fig. 5. Estimation of Installed Power from Rotor Diameter

Estimating Installed Power

Naturally, the angular acceleration of the rotor is limited by the power the electric motor can provide. To pair each simulated rotor with an appropriately sized motor, a benchmarking study was conducted based on existing multicopters (Fig. 5). Fitting a curve to this data yields Eq. 6, which suggests that scaling the installed power with the 3/2 power of the rotor diameter (D) is an adequate estimation.

$$P_{max} = 0.39 D^{1.5} \tag{6}$$

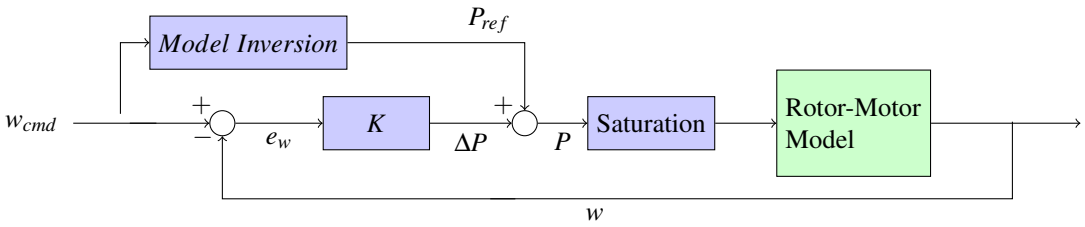

Fig. 6. Control Architecture

Rotor Dynamics Model

The rotational dynamics of the rotor are modeled using conservation of angular momentum (Eq. 7). On the left-hand side is the rate of change of angular momentum, and on the right is the difference between the torque supplied by the motor (modeled as power input divided by rotor speed), and the aerodynamic torque, calculated by the Rensselaer Multicopter Analysis Code (RMAC) (Ref. 11). RMAC uses blade element theory, coupled to a 3x4 Peters-He dynamic wake model, to calculate the phase-averaged rotor forces and moments.

$$I\dot{\Omega} = \frac{P}{\Omega} - \tau_{aero} \tag{7}$$

Rotor heave dynamics are isolated by constraining all but the heave degree of freedom for the system. This is justified because, in hover, the heave dynamics are independent of the longitudinal, lateral, and directional dynamics. Consequently, the heave equation of motion takes the form of Eq. 8, where w is the heave rate of the rotor and T_{rotor} is the thrust produced by the rotor. A mass (m) corresponding to a 2lb/ft^2 disk loading (based on the AeroQuad Cyclone) is used in Eq. 8.

$$m\dot{w} = T_{\text{rotor}} - mg \tag{8}$$

Controller Architecture

This dynamic model constitutes the bare airframe dynamics of the system, and a feedback controller is designed around it to shape the system response, illustrated in Fig. 6. Linear control design is performed such that the closed-loop dynamics are similar on linear approximations of each system, regardless of rotor diameter. This is accomplished via two methods: proportional (state-space pole placement) and proportional-derivative (frequency domain tuning) control of a SISO system. These control laws form the block denoted by K in Fig. 6. In addition to the feedback controller, a feed forward model inversion is included to improve tracking performance of the motor-rotor system. Finally, a saturation block is included to model the physical limitations of the motor considered for each simulation case (estimated using Eq. 6).

Model Validation

The simulation of the isolated rotor was validated using experimental data from the rotor test apparatus at Rensselaer Polytechnic Institute (Fig. 7), which was designed to measure the forces and moments produced by a rotor up to 3 feet in diameter. For the model validation, the open loop response of a 28 inch diameter rotor to a step input in power was recorded.

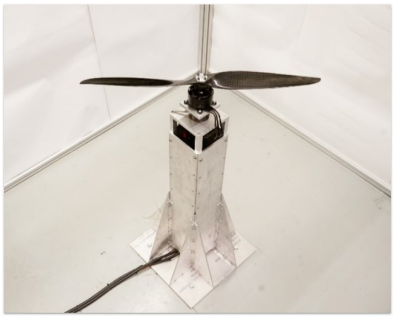

Fig. 7. Rotor Test Apparatus

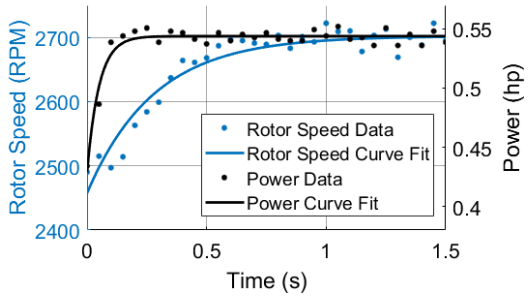

Fig. 8. Experimental Rotor Speed and Power with First Order Curve Fits

Table 3. Rotor Experimental Data Curve Fit Parameters

Response	Time Constant (s)	Time Delay (s)
Motor Power	0.05	0
Rotor Speed	0.28	0.04

A step change in the throttle signal from 23% to 26% received by the ESC at $t = 0.15$ resulted in a rapid change in the mechanical power supplied by the motor from 0.43 hp to 0.54 hp (Fig. 8). Consequently, the rotor speed increased from 2480 RPM to 2700 RPM. Fitting a first-order response (of the form Eq. 2) to both sets of data (Fig. 8) yields the time constant and time delay parameters in Table 3. Based on the relatively low time constant associated with the motor power (18% that of the RPM), it is modeled as an instantaneous change at

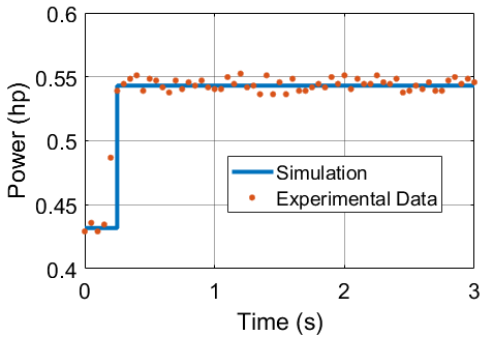

Fig. 9. Power Step Input for Model Validation

$t = 0.15$, as shown in blue on Fig. 9. Using this input, RMAC predicts the change in RPM shown in blue on Fig. 10.

RMAC under-predicts the final rotor speed by around 3.7%, an error consistent with the known behavior of RMAC (Ref. 11), which, similar to other comprehensive analysis codes, tends to over-predict aerodynamic torque. Shifting the simulated response by this constant error (shown by the dotted line in Fig. 10) illustrates the model's ability to capture the transient response, as well as the overall change in rotor speed.

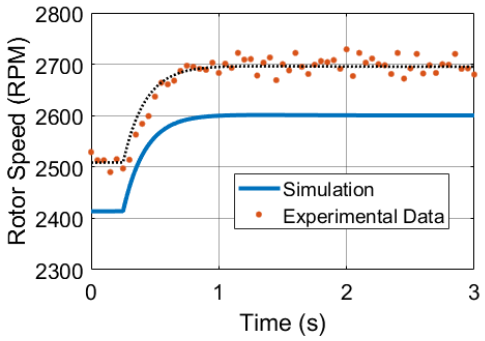

Fig. 10. Open Loop RPM Response for Model Validation

RESULTS

Bare Airframe Response

The bare airframe response was first simulated in order to examine the natural behavior of the system, as well as the effects of increasing rotor rotational inertia. Starting from a steady state hover condition, the power input to the motor was stepped to the value required for a 10 ft/s climb rate at the beginning of the simulation. This power is given as a fraction of the predicted installed power (Eq. 6).

The heave rate responses of the various rotor diameters being considered are shown in Fig. 11. All rotors reach the desired heave rate without any oscillation or overshoot. The change in curvature of the heave rate response for the larger rotors is a result of the increasing rotor rotational inertia.

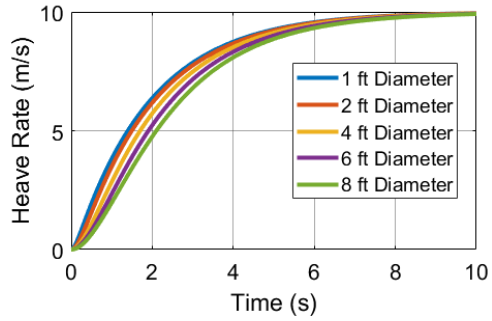

Fig. 11. Open Loop Heave Rate Response

Table 4. Time Constant and Time Delay of Open Loop Responses

Rotor Diameter (ft)	Time Constant (s)	Time Delay (s)
1	1.925	0.063
2	1.986	0.116
4	2.167	0.191
6	2.387	0.247
8	2.626	0.296

A first-order curve is fit to each of the heave responses (as per the ADS-33E-PRF) and the values of the time delay and time constant are calculated using Eq. 2, given in Table. 4. The values are scaled using Eq. 3 and compared to the ADS-33E requirements in Fig. 12. The degradation of handling qualities that occurs with increasing rotor size is a result of the increasing rotor inertia. None of the rotors meet even the scaled Level 2 requirements for the heave rate response, suggesting that open-loop speed control is insufficient for handling qualities purposes, even on small rotors.

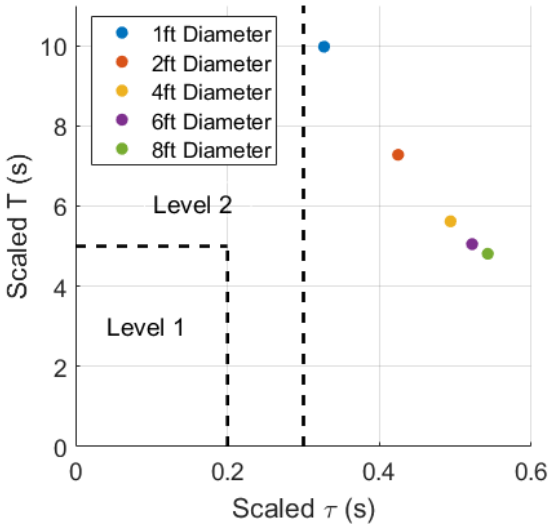

Fig. 12. Open Loop Heave Response Metrics Compared to ADS-33E Requirements

Proportional Control

Because the bare airframe heave dynamics are stable, a proportional gain alone is sufficient to tune the heave response. Due to the presence of the rotational dynamics, the system is second order with two real poles. One pole corresponds to the heave mode while the other corresponds to the rotational dynamics of the motor-rotor system, shown in Fig. 13.

The proportional gain is chosen using pole placement such that the system is critically damped. This design strategy provides the fastest settling time without overshoot, while also providing a predominantly first-order response, per the ADS-33E-PRF standards.

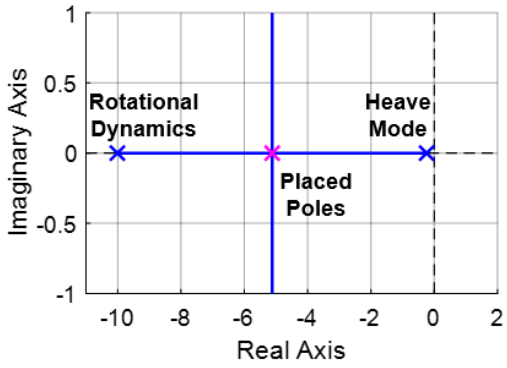

Fig. 13. Root Locus of the 1 ft Rotor with Proportional Control

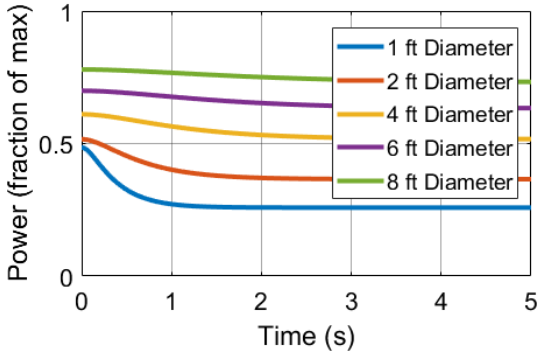

Fig. 14. Input Power with Proportional Control

Starting from a steady hover, a climb rate of 10 ft/s is commanded at $t = 0$. The input power (as a fraction of the installed power) and heave rate response with the proportional controller are shown in Fig. 14 and Fig. 15 respectively. The scaled time constant and delay are compared to the ADS-33E-PRF requirements in Fig. 16. With proportional control alone, only the 1 foot diameter rotor meets the Level 1 requirements. The degradation of handling qualities that occurs with increasing rotor size is a result of the increasing rotor inertia. However, from Fig. 14, it is clear that the use of a proportional gain alone does not utilize the full power capabilities of the motors, indicating that the closed-loop control system can be

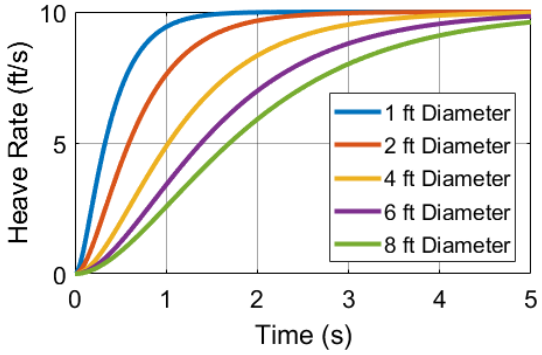

Fig. 15. Heave Rate Response with Proportional Control

redesigned in order to provide a faster response and better satisfy handling qualities metrics. This can be done through the addition of derivative gain.

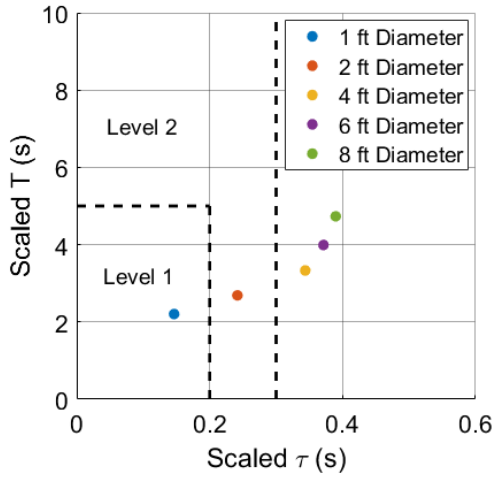

Fig. 16. Heave Response Metrics with Proportional Control Compared to ADS-33E Requirements

Proportional-Derivative Control

The use of a proportional-derivative (PD) controller allows for the further shaping of the heave rate response. If the power constraint is ignored, the rotor responses can be made to match in the time domain. A PD controller is first designed for the 1 foot rotor, such that the closed-loop response is characteristically first-order (no overshoot or oscillation) and the maximum commanded power (at t=0) is equal to the estimated installed power. The PD controllers of the other rotor sizes are then designed such that the closed-loop heave rate response is identical (on the linear models) for all diameters, assuming unlimited power. Comparing the heave response using the nonlinear model (Fig. 17, still ignoring the motor constraint) shows that the linear controllers are equally effective. The power required to achieve this response is shown in Fig. 18 with the exact values of the maximum power given in Table 5. The maximum commanded power for the large rotors greatly exceed the power capacity of their motors, with the largest rotor commanding over 60 times the estimated installed power.

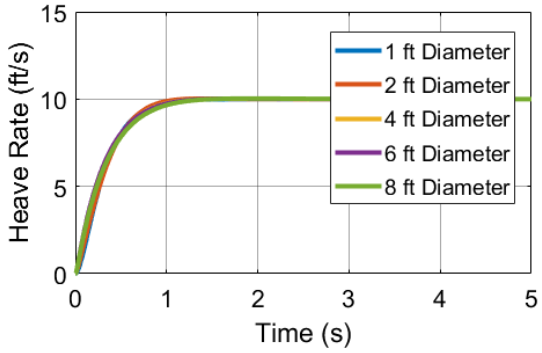

Fig. 17. Heave Rate Response with PD Control, No Power Saturation Limit

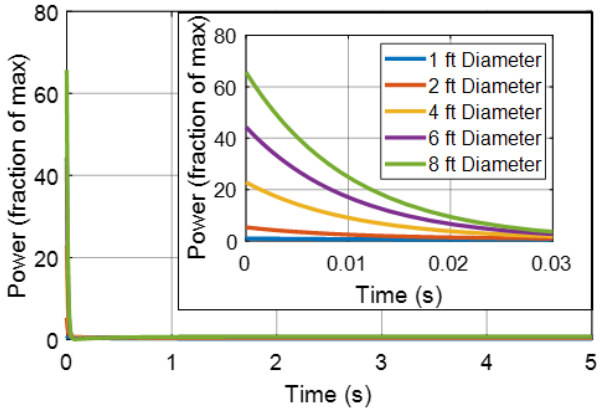

Fig. 18. Input Power with PD Control, No Power Saturation Limit

Table 5. Maximum Commanded Power for Ideal Response

Rotor Diameter (ft)	Maximum Commanded Power (hp)
1	0.4
2	6.2
4	71
6	250
8	590

The simulated heave rate responses presented in Fig. 19 utilize the same controllers used to create the step responses in Fig. 17, but with the inclusion of the power limit. Predictably, restricting the power input to realistic levels slows the system response, with greater lag as the rotor diameter increases. The input power with the saturation limit included is shown in Fig. 20. All of the rotors provide their maximum power at $t = 0$, with larger rotors maintaining this maximum for increasing lengths of time.

The heave rate responses of all the rotor diameters considered meet the ADS-33E-PRF Level 1 requirements (Fig. 21), except for the 8 foot diameter rotor. The limiting factor for the responsiveness of the 8 foot rotor is the time delay (τ) of the heave rate response. This time delay is associated with the initial response of the rotor to a step change in commanded heave rate, while the motor is saturated. Because the motor is

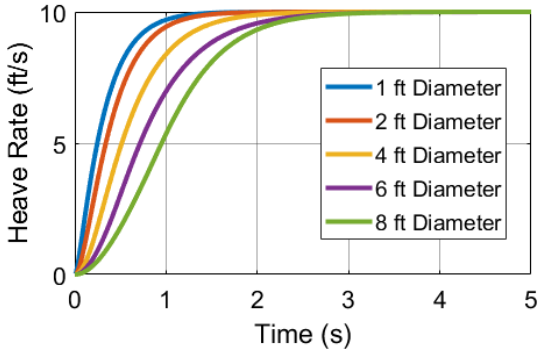

Fig. 19. Heave Rate Response with PD Control

already at its limit, there can be no improvement in the time delay via gain tuning. Thus, the only way an 8 foot diameter rotor can meet the scaled level 1 requirements would be by reducing the inertia of the rotor (via a more complex geometry or less dense material) or by increasing the motor power (and weight).

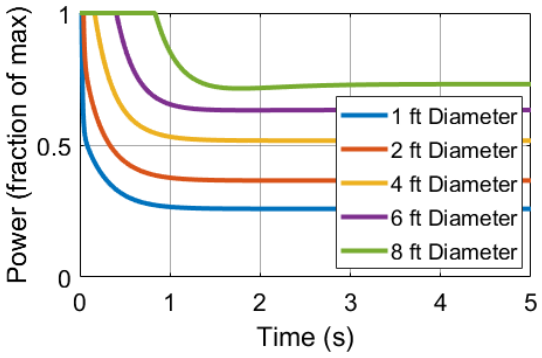

Fig. 20. Input Power with PD Control

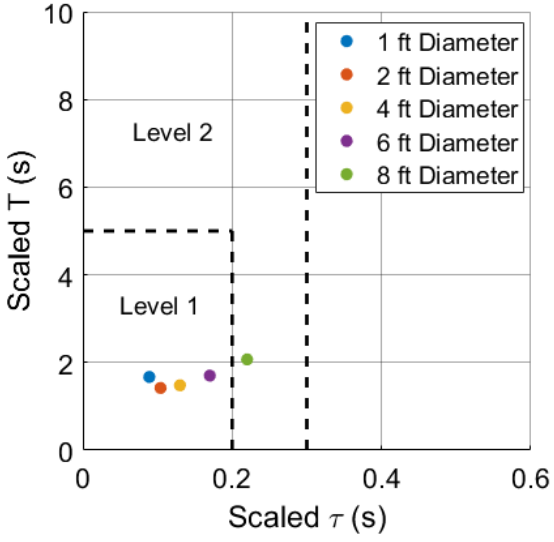

Fig. 21. Heave Response Metrics with PD Control Compared to ADS-33E Requirements

CONCLUSIONS

The effect of rotor radius on the responsiveness of fixed-pitch, variable RPM rotors in heave was explored through simulation. A simple approach based on conservation of angular momentum was found to be sufficient to capture the dynamic response of a rotor in response to a step change in the commanded throttle. Additionally, based on experimental results on a 28 inch diameter rotor, the mechanical power supplied by the motor changed nearly instantaneously, justifying its use as a control input in dynamic simulations.

Due to the natural stability of the heave dynamics, simple proportional control was capable of shaping the response of the heave dynamics, to a degree. However, this was only sufficient for the 1 foot diameter rotor to achieve scaled level 1 handling qualities standards. Including derivative gain allowed greater control and full use of the installed power, allowing rotors up to 6 feet in diameter to meet level 1 requirements. The relative lack of power on the 8 foot diameter rotor caused its time delay to exceed the maximum allowance of the ADS-33E-PRF heave standards, which can only be remedied by changing the design of the rotor or augmenting the motor's capabilities at the expense of weight.

While handling qualities standards are in need of further refinement, preliminary conclusions about the performance of fixed-pitch rotors can be made. Based on the heave dynamics alone, rotors with a diameter of 8 feet or greater will need to reduce the time delay associated with changing the rotor speed, possibly by either increasing the size of the motors (thereby increasing weight), or reducing the rotational inertia (with a more complex blade structure). Alternate configurations could also be considered, such as variable collective pitch which can circumvent the rotational dynamics of the rotor entirely without the need for a swashplate (as no cyclic pitch is required).

REFERENCES

[1]Gipson, L., Dunbar, B., "Urban Air Mobility Grand Challenge," NASA, September 2018, Available: https://www.nasa.gov/uamgc/. [Accessed: December 2018].

[2]"Fast-Forwarding to a Future of On-Demand Urban Air Transportation," UBER Elevate Summit, October 2016.

[3]Johnson, W., Silva, C., and Solis, E., "Concept Vehicles for VTOL Air Taxi Operations," AHS Technical Conference on Aeromechanics Design for Transformative Flight, San Francisco, CA, January 2018.

[4]Ivler, C., Goerzen, C., Wagster, J., Sanders, F., Cheung, K., and Tischler, M., "Control Design for Tracking of Scaled MTE Trajectories on an IRIS+ Quadcopter," AHS International 74th Annual Forum and Technology Display, Phoenix, AZ, May 2018.

[5]Alvarenga, J., Vitzilaios, N., Rutherford, M., Valavanis, K., "Scaled Control Performance Benchmarks and Maneuvers for Small-Scale Unmanned Helicopters," IEEE 54th Annual Conference on Decision and Control, Osaka, Japan, December 2015.

[6]Holmberg, J.A., King, D.J., Leonard, J.R., and Cotting, M.C., "Flying Qualities Specifications and Design Standards for Unmanned Aerial Vehicles," AIAA Atmospheric Flight Mechanics Conference, Honlulu, HI, August 2008.

[7]Cotting, M.C., "Applicability of Human Flying Qualities Requirements for UAVs, Finding a Way Forward," AIAA Atmospheric Flight Mechanics Conference, Chicago, IL, August 2009.

[8]Cotting, M.C., "UAV Performance Rating Scale Based on the Cooper-Harper Piloted Rating Scale," 49th AIAA Aerospace Sciences Meeting, Orlando, FL, January 2011.

[9]Klyde, D.H., Schulze, P.C., Mitchell, D.G., and Alexandrov, N., "Development of a Process to Define Unmanned Aircraft Handling Qualities," AIAA Atmospheric Flight Mechanics Conference, Kissimmee, FL, January 2018.

[10]Anonymous, "Aeronautical Design Standard Performance Specification Handling Qualities Requirements for Military Rotorcraft," Tech Rep., United States Army Aviation and Missile Command, ADS-33E-PRF, March 2000.

[11]Niemiec, R., "Development and Application of A Medium-Fidelity Analysis Code for Multicopter Aerodynamics and Flight Mechanics," Ph. D. Dissertation, Rensselaer Polytechnic Institute, August 2018.